

# Emission Characteristics of A P&W Axially Staged Sector Combustor

Zhuohui J. He<sup>\*</sup>, Changlie Wey<sup>†</sup>, Clarence T. Chang<sup>‡</sup>, Chi Ming Lee<sup>§</sup>, Angela D. Surgenor<sup>\*\*</sup>  
*NASA Glenn Research Center, Cleveland, OH 44135, U.S.A.*

Kristin Kopp-Vaughan<sup>††</sup> and Albert Cheung<sup>‡‡</sup>  
*Pratt & Whitney, East Hartford, CT 06108, U.S.A.*

Emission characteristics of a three-cup P&W Axially Controlled Stoichiometry (ACS) sector combustor are reported in this article. Multiple injection points and fuel staging strategies are used in this combustor design. Pilot-stage injectors are located on the front dome plate of the combustor, and main-stage injectors are positioned on the top and bottom of the combustor liners downstream. Low power configuration uses only pilot-stage injectors. Main-stage injectors are added to high power configuration to help distribute fuel more evenly and achieve overall lean burn yielding very low NO<sub>x</sub> emissions. Combustion efficiencies at four ICAO LTO conditions were all above 99%. Three EINO<sub>x</sub> emissions correlation equations were developed based on the experimental data to describe the NO<sub>x</sub> emission trends of this combustor concept. For the 7% and 30% engine power conditions, NO<sub>x</sub> emissions are obtained with the low power configuration, and the EINO<sub>x</sub> values are 6.16 and 6.81. The high power configuration was used to assess 85% and 100% engine power NO<sub>x</sub> emissions, with measured EINO<sub>x</sub> values of 4.58 and 7.45, respectively. The overall landing-takeoff cycle NO<sub>x</sub> emissions are about 12% relative to ICAO CAEP/6 level.

## I. Introduction

Aircraft nitrogen oxides (NO<sub>x</sub>) emissions can cause problems to the atmosphere, such as smog and ozone in the lower troposphere and decreased ozone in the stratosphere (Wey & Maurice, 2003). Over the past two decades, NO<sub>x</sub> emissions reduction has been a major focus for NASA in aeronautical science research. During the 1990's, NASA's High-Speed-Research (HSR) program focused on developing combustor concepts that reduces NO<sub>x</sub> emissions for supersonic aircrafts. In the 2000's, NASA's Ultra-Efficient-Engine-Technology (UEET) program, Fundamental Aeronautics program, and Advanced Subsonic Technology program found reductions in NO<sub>x</sub> emissions for subsonic aircraft emission. Currently, NASA's Environmentally Responsible Aviation (ERA) project aims to reduce the subsonic aircraft engine NO<sub>x</sub> emissions by 75% with respect to ICAO CAEP/6 level (Chang, Lee, Herbon, & Kramer, 2013). To achieve this goal, NASA is collaborating with fuel injector companies (Woodward, Parker, Goodrich) and engine companies (GE and P&W) to develop state of the art low-NO<sub>x</sub> combustion technologies. Under an ERA project contract, Pratt & Whitney (P&W) developed an axially staged combustor concept, called Axially Controlled Stoichiometry (ACS) combustor, to reduce NO<sub>x</sub> emissions.

Combustion concept designs for commercial aircraft fall into two categories: rich-front-end and lean-front-end. As shown on Figure 1, NO<sub>x</sub> emissions are sensitive to flame temperature. The flame temperature reaches the maximum at equivalence ratio around one. As equivalence ratio departs from stoichiometric, the flame temperature decreases. Rich-Burn Quick-Mixing Lean-Burn (RQL) combustors utilize a rich-front-end designed to reduce NO<sub>x</sub> emissions. In this concept, the combustor front end or primary zone burns fuel rich. In order to minimize NO<sub>x</sub> emissions and complete combustion, this fuel rich combustion mixture is diluted to lean with the quench air jets, minimizing residence time near stoichiometric conditions. A rich primary combustion zone provides a stable flame and a large combustion operability range. Thus, rich-front-end combustors are commonly used in combustor designs.

<sup>\*</sup> Propulsion physicist, *NASA Glenn Research Center*

<sup>†</sup> System Engineer, *NASA Glenn Research Center*

<sup>‡</sup> Engineer, *NASA Glenn Research Center*

<sup>§</sup> Retired Chemical Engineer, *NASA Glenn Research Center*

<sup>\*\*</sup> Engineer, *NASA Glenn Research Center*

<sup>††</sup> Senior Engineer, *Pratt & Whitney*

<sup>‡‡</sup> Senior Engineer, *Pratt & Whitney*

Lean-front-end combustors operate fuel lean throughout the combustor. Most of the combustion air enters through the combustor dome and through fuel injectors or mixing chambers. A minimal amount of air is allocated for cooling. These concepts vary from single fuel injector concepts to multiple fuel injectors in each sector of the combustor. In all concepts, however, the fuel entering the combustor is well mixed with incoming process air and is fuel lean. Lean-front-end concepts require good fuel air mixing to limit local hot spots that generate  $\text{NO}_x$ .

Aircraft engines operate in a wide range power conditions (wide range of pressures, temperatures, and flows). A single fuel injector may not be able to atomize the fuel sufficiently for good fuel-air mixing. As a result, lean-front-end concepts usually involve multiple fuel injection points. In low power conditions, only parts of the fuel injectors are used. This gives local fuel air ratios that are sufficiently high to create continuous stable combustion. In higher power conditions, all fuel injectors are used to distribute fuel more evenly throughout the combustor so one region has high enough fuel air ratios to produce high  $\text{NO}_x$ . The design of the fuel injector system is critical to creating a fuel-lean combustor that is both stable at low power and produces low  $\text{NO}_x$  emissions at high power.

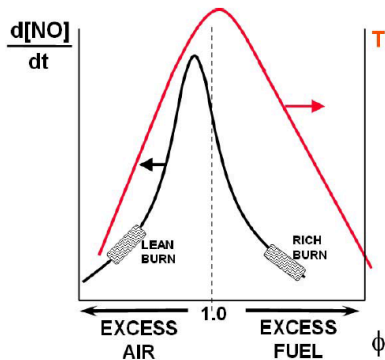


Figure 1: Flame temperature and  $\text{NO}_x$  emissions vs. fuel air equivalence ratio (Samuelsen, 2006).

New aircraft combustor concept screening often starts in a flame-tube test facility, where a fuel injector and accompanying fuel injector cup is tested at various aircraft operational conditions. An example of flame tube test facility is the CE-5 test facility at NASA Glenn Research Center (Bianco, 1995). The fuel-air mixture is injected into a flame tube with a cast ceramic housing. A gas collection probe is placed downstream of the injector at a distance specified to ascertain the fuel injector/ cup configuration's emissions output.

Once a fuel injector/ cup configuration obtains good stability with low  $\text{NO}_x$ , sector combustor test, where three to five fuel injector cups of an aircraft annular combustor is utilized to determine the combustor/ fuel injector module's stability and emissions. In this step, effects of combustor liners and interaction between injector cups are assessed.

In this article, emission characteristics of a three-cup P&W ACS sector combustor are reported. This sector combustor was tested in NASA Glenn Research Center's Advance Subsonic Combustion Rig (ASCR). ASCR is capable of testing combustor hardware at high-pressure conditions up to 60 atm. The main goals of this test are to screen the  $\text{NO}_x$  emissions of this combustion concept at four different ICAO LTO power conditions---taxing (7%), approach (30%), climbing (85%), takeoff (100%)---and to develop  $\text{NO}_x$  emissions correlation equations to use for aircraft engine system level analysis.

## II. Experimental facilities and hardware

### 1. Experimental facilities

The sector combustor test was conducted at the NASA Glenn Advanced Subsonic Combustion Rig (ASCR). A drawing and a picture of the test rig are shown in Figure 2. This test rig can supply nonvitiated air preheated to 975 K at pressure up to 6200 kPa. A venturi meter is used to measure the airflow rate, and turbine meters are used to measure the fuel flow rates. The sector combustor is mounted in a stainless-steel pipe with an 889 mm inside diameter. The combustor section is followed by a water-quench section and backpressure valve. The test rig has four fuel circuits and is capable of on-the-fly mixing JP-8 and alternative aviation fuel at various ratios. The combusted gas samples were collected according to SAE-ARP1256 (SAE international, 2011) and analyzed according to the

standard gas-analysis procedure, SAE-ARP1533 (SAE International, 2004). CO, CO<sub>2</sub>, O<sub>2</sub>, NO<sub>x</sub>, and unburned hydrocarbons (UHC) are measured. The combustor rig has diagnostic windows along the combustor section, which could be used for laser diagnostic, or visual fuel leak detection. Dynamic pressures are measured upstream ( $P_3$ ) and inside ( $P_4$ ) the combustor.

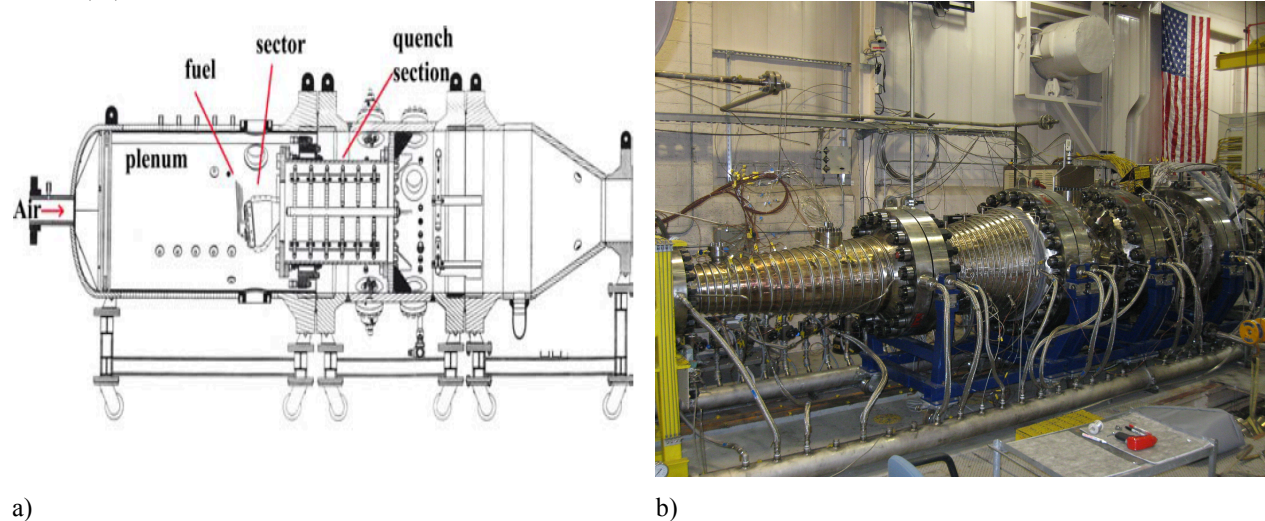


Figure 2: a) Drawing and b) picture of ASCR test facility in NASA Glenn Research Center.

## 2. Sector combustor hardware

The ACS sector combustor hardware was developed by P&W under the NASA ERA project. This sector combustor is a three-cup sector. A basic drawing of each injector cup is shown in Figure 3a. Like a previous P&W axially staged combustor (Figure 3b), fuel injection splits into two stages: pilot and main. Pilot-stage injectors are located on the front dome plate of the combustor, and main-stage injectors are positioned on the top and bottom of the combustor liners downstream. There are two fuel injection configurations. Low power configuration only uses pilot-stage injectors, while high power configuration utilizes both pilot-stage and main-stage fuel injectors. As discussed previously, this allows for stable and efficient combustion with low NO<sub>x</sub> emissions through the entire aircraft operability envelope.

To account handle the staging, three fuel circuits are used in this test. One fuel circuit supplies fuel to the main fuel injectors. Two fuel circuits serve the pilot stages injectors. These circuits allow for individual fueling of off circuits.

In order to determine if the configuration obtains efficient burning and low NO<sub>x</sub> emissions a collection system of probes was attached to the exit of the combustor. Nine picalo probes are placed at the exit of the combustor to collect combustion products for gas analysis. The probes were water cooled in order to protect the hardware and quench any additional CO oxidation.

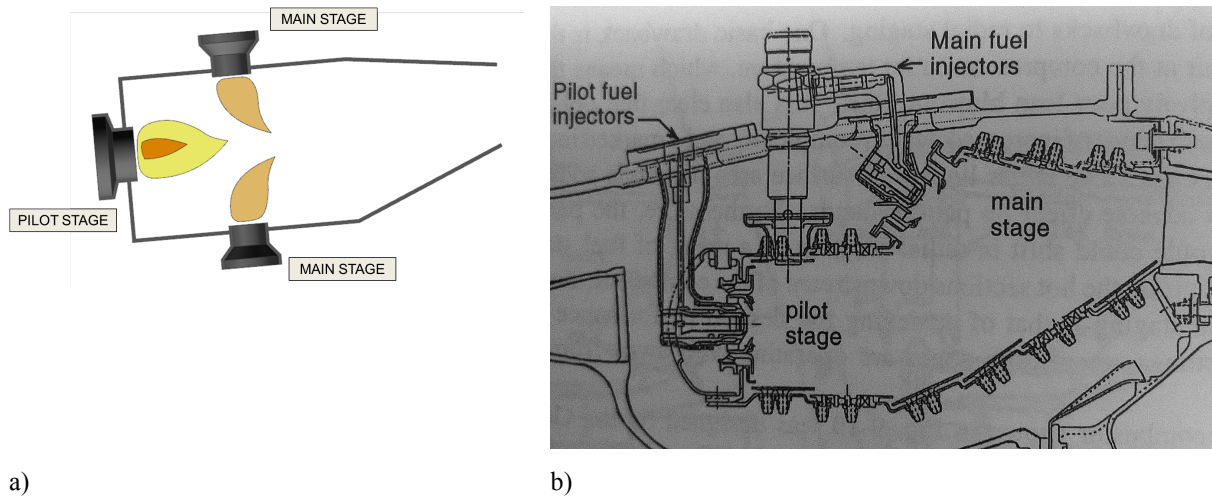


Figure 3: a) ASC combustor cross-section view. b) P&W V2500-AS combustor (Lefebvre, 1998).

### III. Results and Discussion

#### 1. Low Engine Power Configuration

For low power the overall equivalence ratio is low, and only the pilot-stage injectors are used for fuel injection. Pilot-stage injectors inject fuel through the front dome plate of the combustor. The combustor front-end or pilot zone is designed to have relatively high local fuel air ratio at some locations. This provides a stable pilot combustion zone to prevent lean blow out, combustion instabilities, and to assure efficient combustion. A nominal amount of air enters the combustor through the fuel nozzle cup in order to obtain sufficient stoichiometry to allow for a stable pilot zone. Additional process air enters through the main fuel injector cups, but not fuel is supplied to the main fuel injectors for low power. The remaining air is used for liner cooling.

The combustor temperature profile for the low power configuration is similar to a rich-front-end combustor as shown in Figure 4. The flame temperature is low near the dome. As the fuel-rich combusted gas moves forward, the flame temperature increases then decreases quickly as the fuel-rich combusted gas dilutes with air from the main air swirlers and the front-end liners. The  $\text{NO}_x$  emissions at the combustor front-end and back-end are low due to low flame temperature that greatly reduces thermal  $\text{NO}_x$ . In addition, oxygen depletion at the combustor front-end would reduce the  $\text{NO}_x$  production in that zone (Lefebvre, 1998). The hot zone in between the front-end and back-end only occupies small portion of the combustor making the residence time in that zone very low. The middle zone, however, may create the most  $\text{NO}_x$  emissions because it has sufficient temperature and oxygen to do so. The time spent in the middle zone between from front-end and back-end, therefore largely dictates the overall  $\text{NO}_x$  emission during low power operation. As shown in Figure 5a, the  $\text{EINO}_x$  values for low power configuration increase and then decrease before and after overall fuel air equivalence ratio around 0.14. This indicates the middle zone has the most flame locations whose stoichiometry is near stoichiometric at this overall fuel air equivalence ratio. Influence of fuel air equivalence ratio on the  $\text{NO}_x$  emissions before and after overall  $\Phi$  of 0.14 are respectively about  $\Phi^{3.2}$  and  $\Phi^{-2.15}$ . An influence coefficient greater than zero indicated an increase in overall  $\Phi$  would increase  $\text{NO}_x$  emissions, and an influence coefficient of less than zero indicates an increase in overall  $\Phi$  would tend to decrease the  $\text{NO}_x$  emissions. The  $\text{NO}_x$  emissions trend is expected to change again at much higher overall fuel air ratio because as the overall fuel air ratio is raised, the combustor back-end flame temperature would increase. When the  $\text{NO}_x$  emissions in the combustor back-end become more significant than the combustor front-end, and the overall  $\text{NO}_x$  emissions would increase as overall fuel air equivalence ratio increases. This phenomenon is seen in Figure 5b, idle condition  $\text{NO}_x$  and CO emissions vs. effective pilot zone equivalence ratio. The data in Figure 5b was collected with the same hardware at UTRC Jet Burner Test Stand (JBTS) facility.

Figure 5a also shows that the  $\text{NO}_x$  emissions increase as inlet air temperature ( $T_3$ ) and pressure ( $P_3$ ) increase. Influence of inlet air pressure on the  $\text{NO}_x$  emissions is in between  $P_3^{0.25}$  to  $P_3^{0.50}$ . It is small when comparing to influence of inlet air temperature, which is an exponential function of  $T_3/175$ .

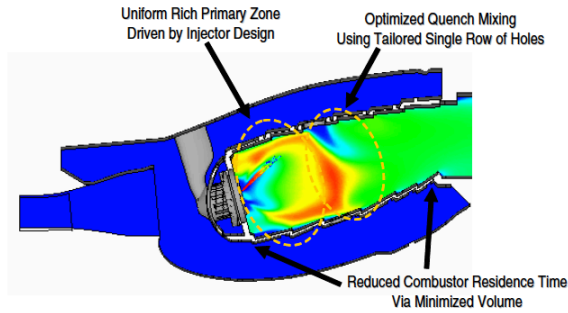
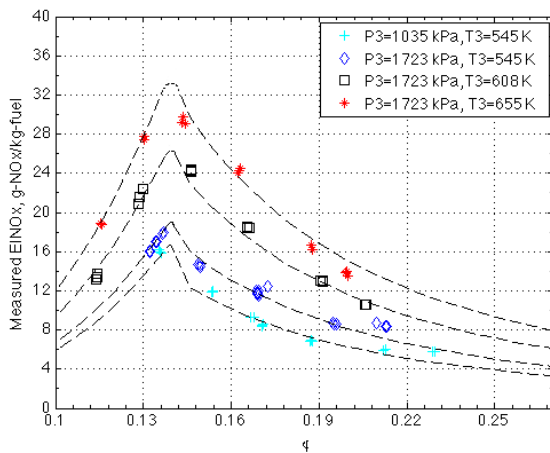
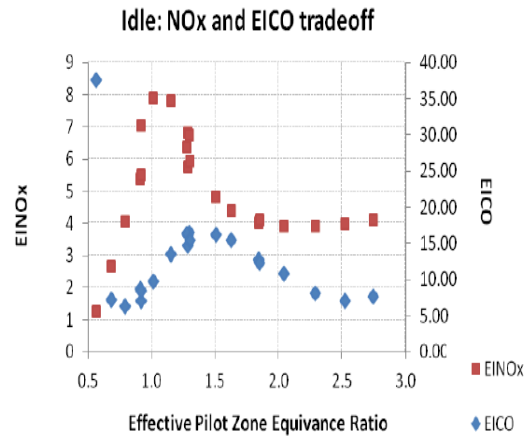


Figure 4: temperature profile for the P&W TALON RQL combustor (McKinney, Sepulveda, Sowa, & Cheung, 2007).



a)



b)

Figure 5: a) Low engine power configuration,  $EINO_x$  vs.  $\Phi$ , b)  $EINO_x$  and  $EICO$  vs. effective pilot zone equivalence ratio (Pratt & Whitney, 2012).

Figure 6 shows carbon monoxide (CO) and unburned hydrocarbon (UHC) emissions for the low power configuration. The CO emission is much greater than the UHC emission, as expected with combustors designed to good combustion efficiency. As shown in Figure 5b and Figure 6a, the CO emission increases until overall equivalence ratio of 0.16, then becomes steady and slowly decreases as fuel air equivalence ratio goes up. On the other hand, UHC emission decreases as equivalence ratio increases (Figure 6b). For low power configuration, CO and UHC are mainly generated at combustor front end, where oxygen is depleted. Most of these CO and UHC then oxidize by dilution air to  $CO_2$  before exiting the combustor as the combustion process is completed. The amount of CO and UHC that remains at the end of the combustor depends on how much CO and UHC were generated in the primary zone and the oxidation rates of CO and UHC later in the combustor and residence time. The longer the residence time the lower the CO may be, but the higher the  $NO_x$  may become. This combustor was designed to minimize CO, UHC, and  $NO_x$  emissions. This can only be achieved by controlling both the residence time and the temperature (as the oxidation rates of CO, UHC, and  $NO_x$  increases at different rates with temperature). As shown in Figure 5a,  $EICO$  value increases before equivalence ratio of 0.16. This might be due to lack of oxygen in the combustor front-end that generates high level of CO and low flame temperature after the combustor front-end, which leads to low CO oxidation rate. As the overall fuel air equivalence rate increases, combustor back-end flame temperature increases; the  $EICO$  value becomes steady and then decreases as combustion back-end flame temperature gets higher. Both CO and UHC have similar effects by inlet air temperature and pressure. Increasing



inlet air temperature and pressure will help decrease CO and UHC emissions. Even at the peak of CO and UHC, the emissions remained fairly low.

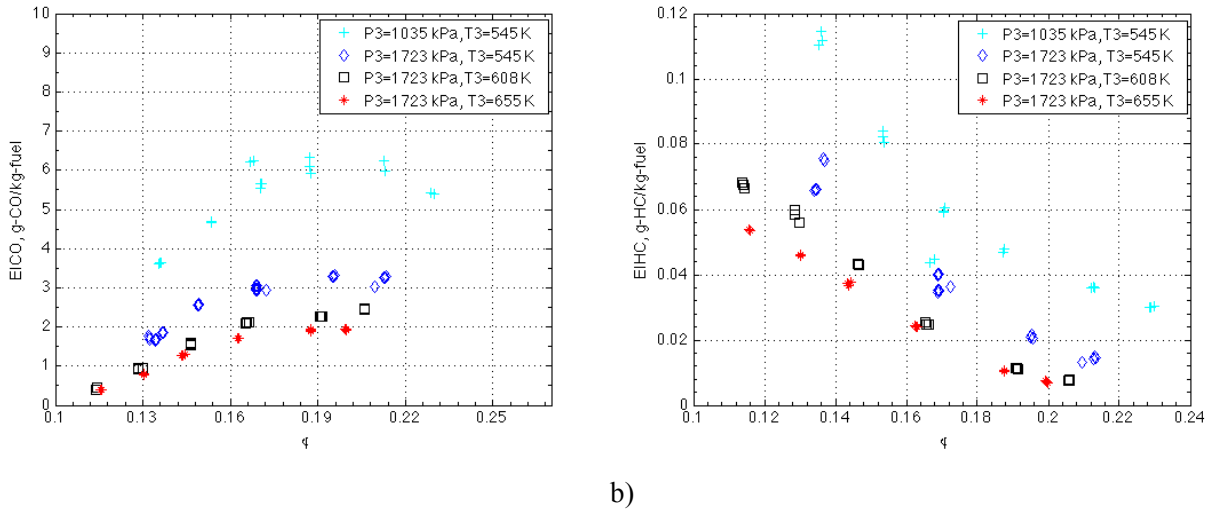


Figure 6: Low power configuration a) CO and b) UHC emissions.

## 2. High Engine Power Configuration

For higher power configuration, both pilot-stage and main-stage injectors are fueled. Main-stage injectors are located axially downstream of the pilot-stage injectors on both the OD and ID of the combustor. There are several advantages of this combustor design. First, with more fuel injection points, fuel and air are able to mix more evenly throughout the combustor and achieve overall lean burn without any pockets of unmixedness (which can lead to high temperatures and high NO<sub>x</sub> emission). Second, the main-stage injectors are position downstream of the pilot injectors. Airflow through main-stage injectors does not affect the swirl-stabilized pilot zone, which is important for combustion flame stabilities (Pratt & Whitney, 2012). Third, higher upstream temperature make the main-stage fuel burn efficiently, even with a low residence time. The ability to burn efficiently with a low residence time assures low CO, UHC, and NO<sub>x</sub> emissions. This is of particular importance because most of the fuel injected at high power conditions comes from the main stage.

High power configuration emission characteristics are similar to many lean burn concepts that tested previously at NASA Glenn Research Center. Figure 7 shows the NO<sub>x</sub> emissions as a function of overall equivalence ratio (local pilot  $\Phi$  stays at 0.6). The influence of inlet air temperature and pressure are similar to the low power configuration, with  $P_3^{0.374}$  and  $e^{T_3/175}$ . The high power configuration has lower NO<sub>x</sub> emissions than the low power configuration. This may be because there are little or no pockets of near stoichiometric burner for this the well mixed mains (which is where most of the fuel is being added). The EINO<sub>x</sub> emissions value at  $P_3 = 2000$  kPa,  $T_3 = 655$  K, and  $\Phi=0.3$  is about 7 for low power configuration, while high power configuration EINO<sub>x</sub> emissions value is about 1. EINO<sub>x</sub> emissions are a power function of fuel air equivalence ratio, with  $\Phi^{4.62}$ . The high  $\Phi$  dependence for lean combustion has been observed before in a NASA 9-points LDI concept with 45° air swirlers ( $\Phi^{5.07}$ ). That study showed that the swirl angle had a determining factor on the influence coefficient for  $\Phi$ . CDF studies suggested a 45° swirler does not allow for a strong central recirculation zone, but a flow field with increased swirl angle (which showed a lower dependence on  $\Phi$ ) did have a strong central recirculation zone. (Kumud, Mongia, & Lee, 2013). The surface area of the flame that is outer recirculation zone stabilized may be greater than an inner circulation zone stabilized flame, and this could lead to higher influence of  $\Phi$ .

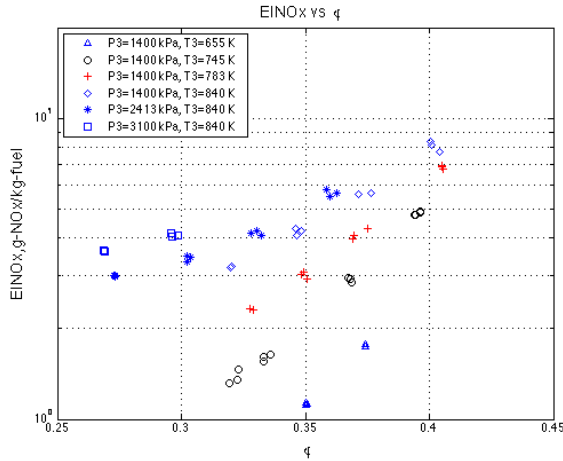
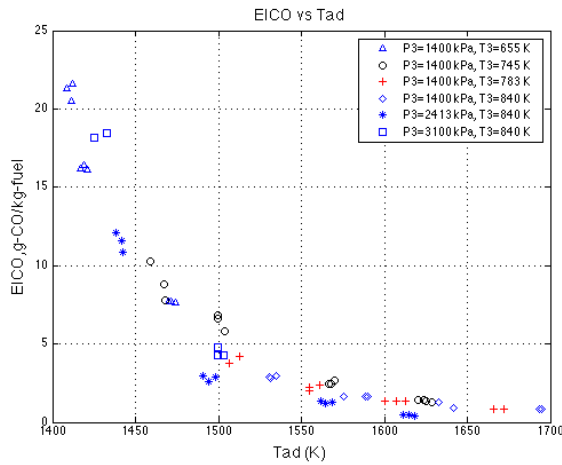
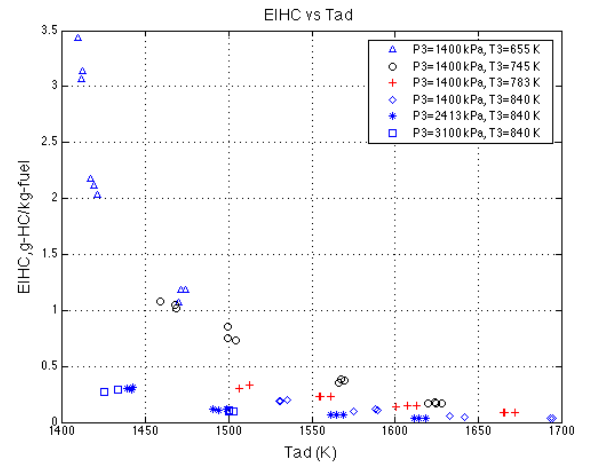


Figure 7: high power configuration  $\text{NO}_x$  emission.

Figure 8 shows the CO and UHC emissions vs. the average calculated adiabatic flame temperature. Emission trends for both UHC and CO are similar and heavily affected by the calculated adiabatic flame temperature. As the calculated adiabatic flame temperature increases, CO and UHC emissions decrease and become steady at around calculated adiabatic flame temperature of 1500 K. Similar trend is seen with NASA's 9-points LDI injector (Tacina, Lee, & Wey, 2005). Lower flame temperature leads to slower CO and UHC oxidation rate. As a result, CO and UHC emissions are lower at higher flame temperature. Inlet air pressure of 2413 kPa or higher also reduces UHC emission, especially at calculated adiabatic flame temperature lower than 1500 K. Improvement in CO emission is not obvious at these conditions. This may be due to the fact that the flame temperature and residence time was sufficiently high for good CO oxidation over this regime.



a)



b)

Figure 8: high power configuration a) CO and b) UHC emissions.

The fuel-split ratio between pilot-stage and main-stage injectors affects both  $\text{NO}_x$  emissions and combustion efficiency for the high power configuration. As shown in Figure 9, a higher local pilot zone fuel air equivalence ratio will increase  $\text{NO}_x$  emissions while CO emissions are decreased. As the local pilot zone equivalence ratio increases

from 0.67 to 0.95, the  $EINO_x$  value increase from 2.4 to 10, and  $EICO$  decreases from 1.6 to 0.6. This result might be due to two factors: flame temperature and residence time. More fuel injected through pilot-stage injector gives higher combustor front-end flame temperature and longer residence time, which would decrease CO emission and increase  $NO_x$  formation, while injecting more fuel through main-stage injector would have the opposite effects. The pilot also designed to be somewhat less well mixed than the main stage. This is important for combustion stability; however less mixed regions of the flow create higher equivalence ratios creating higher temperatures. Any increase in %mass of fuel to the pilot would therefore results in a higher % of near stoichiometric regions causing an increase in  $NO_x$  and a decrease in CO emissions. While low  $NO_x$  and CO are crucial to an low emissions combustor, the ability to change the stoichiometry of the pilot and main zones on the fly can aid in the operability and performance of the combustor. Testing stoichiometry splits and understanding the emissions impact is crucial to the design of a new combustor.

After mapping the operability envelope a set point can be chosen for the main and pilot zone fuel split. This choice was set based on low  $NO_x$ , CO, and UHC, emissions as well as good combustion stability and margin to any stability boundary. The lowest pilot  $\Phi$  that obtains stable combustion is not necessarily a robust design for operability. For high power a pilot zone  $\Phi=0.6$  was chosen and the remaining fuel was provided to the main fuel injectors.

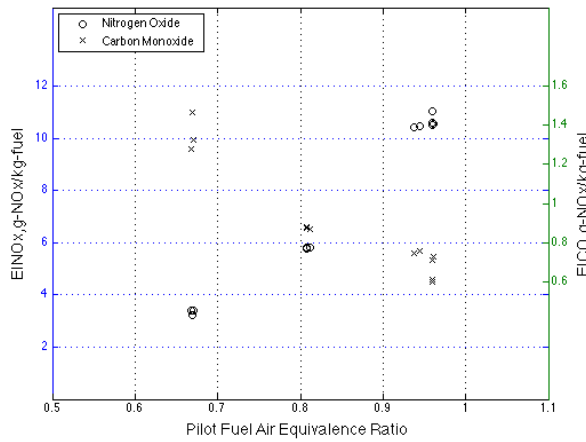


Figure 9: effect of fuel split ratio on  $NO_x$  and CO emissions.

### 3. $EINO_x$ emissions correlation equations

The three  $EINO_x$  emissions correlation equations listed in Table 1 were developed using the data shown in Figure 4 and Figure 6. For the high power configuration, the local pilot zone equivalence ratio stays at 0.6.  $EINO_x$  emissions are a function of inlet air pressure ( $P_3$ ), inlet air temperature ( $T_3$ ), and equivalence ratio ( $\Phi$ ). The method used in developing these equations is described in a previous study on Parker Hnnifin's multipoint LDI injector (He, Chang, & Follen, 2014). The experimental  $EINO_x$  data is plotted against calculated  $EINO_x$  data in Figure 10. The R-square values are 0.962 or higher.  $EINO_x$  dependency on  $P_3$  is small, which ranges from  $P_3^{0.25}$  to  $P_3^{0.50}$ , and it is an exponential function of  $T_3/175$ . The greatest change is on the fuel air equivalence ratio dependence, which ranges from  $\Phi^{-2.15}$  to  $\Phi^{4.62}$ . The ability to collapse all of the high power data into a single equation may be due to the fact that the pilot equivalence ratio remained constant. This may indicate that the pilot zone has the largest impact of emissions. A pilot  $\Phi$  of 0.5 was also tested, but not included in the correlation because it was judged as less superior than the  $\Phi=0.6$  case for overall operability. Data from the  $\Phi=0.5$  case is presented in the next section of this paper.



Table 1: EINO<sub>x</sub> emissions correlation equations.

Engine Power Conditions	NO <sub>x</sub> Correlation equations
1) Low power configuration ( $\Phi < 0.14$ )	$EINO_x = 76.45 * P_3^{0.25} * e^{\frac{T_3}{175}} * \Phi^{3.2}$
2) Low power configuration ( $\Phi > 0.14$ )	$EINO_x = 0.000237 * P_3^{0.50} * e^{\frac{T_3}{175}} * \Phi^{-2.15}$
3) High power configuration ( $\Phi > 0.30$ )	$EINO_x = 0.36 * P_3^{0.374} * e^{\frac{T_3}{175}} * \Phi^{4.62}$

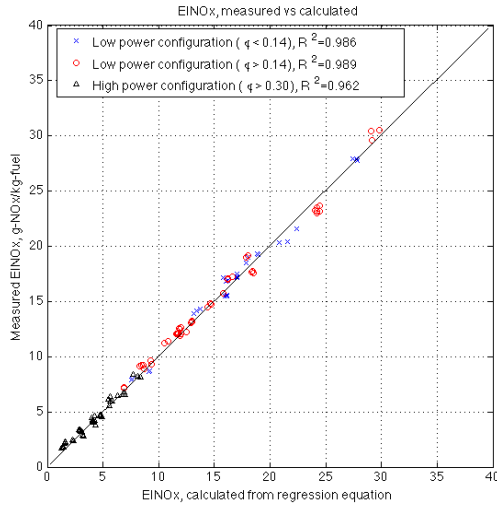


Figure 10: measured EINO<sub>x</sub> emissions vs. calculated from correlation equations.

#### 4. ICAO landing-takeoff (LTO) EINO<sub>x</sub> emissions

The ACS combustor NO<sub>x</sub> emissions at four ICAO LTO power conditions were assessed in this test, and the EINO<sub>x</sub> values are listed in Table 2. For the 7% and 30% engine power conditions, NO<sub>x</sub> emissions are obtained with the low power configuration, and the EINO<sub>x</sub> values are 6.16 and 6.81. The high power configuration was used to assessed 85% and 100% engine power NO<sub>x</sub> emissions. Two different fuel staging are tested, one with local pilot zone  $\Phi$  stays at 0.5 and another with local pilot zone  $\Phi$  stays at 0.6. NO<sub>x</sub> emissions at 85% and 100% engine power conditions were experimentally assessed in ASCR with high power configuration (local pilot zone  $\Phi = 0.5$ ). The EINO<sub>x</sub> values are 4.58 and 7.45. Along with the 7% and 30% engine power NO<sub>x</sub> emissions, the overall landing-takeoff cycle NO<sub>x</sub> emissions are about 12% relative to ICAO CAEP/6 level. As discussed previously in this paper, although a pilot  $\Phi=0.5$  gives good emissions and operability, there may be less margin than desired over the entire operating envelope.

For high power configuration (local pilot zone  $\Phi = 0.6$ ), highest inlet air pressure and temperature tested in ASCR are 3100 kPa and 810 K respectively. Further testing was limited due to a potential fuel leak in the sector combustor hardware. Using the high power configuration correlation equation, the 85% and 100% engine power NO<sub>x</sub> emissions (local pilot zone  $\Phi = 0.6$ ) are estimated as 9.12 and 14.52. The percentage reduction relative to

ICAO CAEP/6 is 83 percent. This is significant because this large reduction comes with a design that was found to be stable and flexible with fuel splits, which improved overall operability.

Table 2: ICAO landing-takeoff (LTO) EINO<sub>x</sub> emissions

ICAO engine power Conditions	Pilot local $\Phi = 0.5$	Pilot local $\Phi = 0.6$
<b>7%</b>	6.16	6.16
<b>30%</b>	6.81	6.81
<b>85%</b>	4.58	9.12
<b>100%</b>	7.45	14.52
<b>Reduction relative to CAEP/6</b>	88%	83%

#### IV. Summary

The emission results of P&W Axially Controlled Stoichiometry (ACS) sector combustor are presented in this article. Multiple injection points and fuel staging strategies are used in this combustor design. The low power configuration uses only pilot-stage injectors. Main-stage injectors are added to high power configuration to help distribute fuel more evenly and achieve overall lean burn yielding very low NO<sub>x</sub> emissions. With this advantage, high power configuration NO<sub>x</sub> emissions index are lower than for the low power configuration. NO<sub>x</sub> emissions for this combustor concept were assessed experimentally at NASA Glenn Research Center's Advance Subsonic combustion Rig over the entire operating range of the LTO cycle. This ACS combustor design meets the ERA program goal in reducing NO<sub>x</sub> emissions while maintaining high combustion efficiency and flame stability. The ICAO landing-takeoff NO<sub>x</sub> emissions are verified to be 88% under the ICAO CAEP/6 standard, exceeding the ERA project goal of 75% reduction, and the combustor proved to have stable combustion with room to maneuver on fuel flow splits for operability.

#### Acknowledgments

This project was funded by NASA's Environmentally Responsible Aviation (ERA) program.

## References

- Bianco, J. (1995). NASA Lewis Research Center's combustor test facilities and capabilities. *AIAA-1995-2681* .
- Chang, C. T., Lee, C., Herbon, J. T., & Kramer, S. K. (2013). NASA Environmentally Responsible Aviation Project Develops Next- Generation Low-Emissions Combustor Technologies (Phase I). *Aeronautics & Aerospace Engineering* , 2 (4).
- He, Z. J., Chang, C. T., & Follen, C. E. (2014). NO<sub>x</sub> Emissions Performance and Correlation Equations for a Multipoint LDI Injector. *NASA/TM—2014-218116* .
- Kumud, A., Mongia, H., & Lee, P. (2013). CEF Best Practices To Predict NO<sub>x</sub>, CO and Lean Blowout for Combustor Design. *ASME Turbo Expo 2013*. San Antonio, Texas, USA.
- Lefebvre, A. H. (1998). *Gas Turbine Combustion* (2nd ed.). Philadelphia: Taylor and Francis.
- McKinney, R. G., Sepulveda, D., Sowa, W., & Cheung, A. K. (2007). The Pratt & Whitney TALON X Low Emissions Combustor: Revolutionary Results with Evolutionary Technology. *45th AIAA Aerospace Sciences Meeting* (pp. AIAA 2007-386). Reno, Nevada: AIAA.
- Pratt & Whitney. (2012). *NASA N+2 ADVANCED LOW NO<sub>x</sub> COMBUSTOR TECHNOLOGY-Final Report*. East Hartford: Pratt & Whitney.
- SAE International. (2004). Procedure for the Analysis and Evaluation of Gaseous Emissions from Aircraft Engines. SAE/ARP1533, 2004-07.
- SAE international. (2011). Procedure for the Continuous Sampling and Measurement of Gaseous Emissions from Aircraft Turbine Engines. SAE ARP1256D, 2011-07.
- Samuelson, S. (2006). Rich Burn, Quick-Mix, Lean Burn (RQL) Combustor. In N. E. Laboratory (Ed.), *The Gas Turbine Handbook*. U.S. Department of Energy, Office of Fossil Energy.
- Tacina, R., Lee, P., & Wey , C. (2005). A Lean-Direct-Injection Combustor Using A 9 Point Swirl-Venturi Fuel Injector. *ISABE-2005-1106*.
- Wey, C., & Maurice, L. Q. (2003). Exploring Aviation's Environmental Impact. *AIAA-2003-5993* .